Jpn. J. Cancer Res. **91**, 1211–1221, December 2000

Isolation of Differentiated Squamous and Undifferentiated Spindle Carcinoma Cell Lines with Differing Metastatic Potential from a 4-Nitroquinoline N-Oxide-induced Tongue Carcinoma in a F344 Rat

Shinichi Takeuchi,[1,2] Hayao Nakanishi,[1,5] Kenji Yoshida,[2] Shinji Yamamoto,[3] Hidefumi Tonoki,[4] Takahisa Tsukamoto,[2] Shoji Fukushima,[3] Tetsuya Moriuchi,[4] Kenichi Kurita[2] and Masae Tatematsu[1]

[1]Laboratory of Pathology, Aichi Cancer Center Research Institute, 1-1 Kanokoden, Chikusa-ku, Nagoya 464-8681, [2]First Department of Oral and Maxillofacial Surgery, School of Dentistry, Aichi-Gakuin University, 2-11 Suemori-dori, Chikusa-ku, Nagoya 464-8651, [3]Department of Pathology, Osaka City University Medical School, 1-4-54 Asahi-machi, Abeno-ku, Osaka 545-8585 and [4]Division of Cell Biology, Cancer Institute, Hokkaido University School of Medicine, N-17 W-5, Kita-ku, Sapporo 060-8638

One differentiated squamous cell carcinoma (SCC) cell line (RSC3-E2) and two undifferentiated tumor cell lines (RSC3-LM and RSC3-E2R) with different metastatic potential were established from a 4-nitroquinoline N-oxide (4NQO)-induced differentiated SCC in F344 rat tongue. The RSC3-E2 subline was isolated from a parental cell line (RSC3-P) by single cell cloning *in vitro*, whereas the RSC3-LM subline was isolated from a lung metastatic focus after subcutaneous (s.c.) injection of RSC3-P cells. The RSC3-E2R cell line was isolated from a lung metastatic focus following s.c. injection of RSC3-E2 cells after X-irradiation *in vitro*. The RSC3-E2 cell line is keratin-positive and grows as a keratinizing tumor in nude mice, whereas RSC3-LM and RSC3-E2R cells are keratin-negative, vimentin-positive and form undifferentiated tumors. When s.c. injected into nude mice, the RSC3-E2 cell line proved to be non-metastatic, while the RSC3-LM cell line was metastatic by both hematogenous and lymphogenous routes, and the RSC3-E2R cell line was metastatic only hematogenously. *In vitro* relative growth rates and *in vitro* invasion activity of these cell lines were in the order RSC3-LM>RSC3-E2R>RSC3-E2. Chromosome analysis revealed two peaks with modal chromosome numbers of 83 and 78 for RSC3-P cells and single peaks at 83, 78 and 56 for RSC3-LM, RSC3-E2 and RSC3-E2R cell lines, respectively. Common structural abnormalities on chromosome 11 were shared by all cell lines. Mutation analysis of the *p53* gene using a yeast functional assay demonstrated RSC3-LM cell line to have a point mutation at codon 269, whereas RSC3-E2 and RSC3-E2R had double mutations at codons 106 and 170 on each allele. These results suggest that the two undifferentiated RSC3-LM and RSC3-E2R tumor cell lines with different metastatic potential were generated from differentiated SCC cells via different genetic pathways as a consequence of tumor progression *in vivo* and *in vitro*, respectively. These cell lines should provide a useful model for understanding mechanisms of hematogenous and lymphogenous metastasis, as well as tumor progression of oral SCCs.

Key words: 4NQO — Rat tongue carcinoma — Spindle cell tumor — Tumor progression — Lymph node metastasis

Cancer of the oral cavity is a very common disease throughout the world,[1)] with squamous cell carcinomas (SCCs) as clinically the most significant malignant neoplasms. SCCs arising in the oral cavity account for approximately 50% of all head and neck cancers.[2)] Although new operative techniques and adjuvant measures such as chemotherapy and radiotherapy against oral SCCs have progressed, patients with advanced oral SCCs still have a poor prognosis, with a 5-year survival rate of less than 30%.[3)] Currently, the most important factor in determining the prognosis of patients with SCCs of the oral cavity is metastasis to the cervical lymph nodes.[4)] Regional lymph node metastasis and distant-organ metastasis occur from relatively early stages of development of primary tumors, because of the abundance of blood and lymph vessels, particularly in tongue carcinomas.[5)] An undifferentiated spindle carcinoma, an extreme form of oral SCC and an entity well recognized to be highly metastatic, is also clinically and prognostically important, since it may occur as a consequence of tumor progression, sometimes after radiation therapy,[6)] and its prognosis is very poor.[7)] To date, however, mechanisms of metastasis and tumor progression to undifferentiated type oral SCCs remain essentially unclear.

[5] To whom correspondence should be addressed.
E-mail: hnakanis@aichi-cc.pref.aichi.jp

To gain further insight into human oral cancer metastases and progression, experimental *in vivo* models that mimic the natural course of the disease progression are essential. Although many human oral carcinoma cell lines are available, most of them have a low rate of spontaneous metastasis, if any.[8, 9] Much information on the carcinogenesis and progression of oral SCCs has been obtained from experimental animal models such as 9,10-dimethyl-1,2-benzanthracene (DMBA)-induced buccal pouch carcinogenesis in hamsters[10, 11] and 4-nitroquinoline 1-oxide (4NQO)-induced tongue carcinogenesis in rats.[12, 13] The alkylating agent 4NQO is a powerful carcinogen in several organs, and tongue SCCs can be specifically induced by its application of low concentrations in the drinking water.[12] The 4NQO-induced rat SCC is an excellent model for studies of early events in oral carcinogenesis, because progression of premalignant lesions to SCCs is similar to that in the human situation,[13] and several differentiated SCC cell lines in culture have already been established.[14–16] Models for later events associated with tumor progression and metastasis of oral SCCs, however, are quite few in number. Undifferentiated carcinoma cell lines derived from spindle cell tumors formed after transplantation of 4NQO-induced epithelial cell lines into nude mice are examples of useful metastasis models, but their biological characteristics remain to be elucidated.[17, 18]

In the present study, we established a differentiated SCC cell line and undifferentiated tumor cell lines from a 4NQO-induced rat tongue carcinoma. They show variation in metastatic potential with regard to hematogenous, lymphogenous and peritoneal dissemination. Their growth, invasion, differentiation, cytogenetic and *p53* tumor suppressor gene status were examined with the aim of casting light on the mechanisms underlying phenotypic shift from differentiated, non-metastatic SCC to undifferentiated, metastatic tumor cells.

MATERIALS AND METHODS

Source of cell lines SCCs of the rat tongue were induced by a previously reported procedure.[19] In brief, three 6-week-old male F344 rats (Japan SLC, Inc., Hamamatsu) were given 20 ppm 4NQO in their drinking water for 16 weeks. They were then maintained on top water and basal diet. Oral tumors became visible on the mucosa of the tongue from 24 weeks after the start of the experiment. Individual tumors were papillary nodules, approximately 5 mm in diameter and localized in the posterior part of the dorsum linguae. Rats were killed by ether anesthesia for removal of tumors. Half of each fresh tumor was used for preparation of cells in primary culture. The remaining tissue was fixed in 10% buffered formalin, embedded in paraffin and sectioned for histopathological assessment with hematoxylin and eosin staining.

Establishment of cell lines The fresh tumor tissues were washed with Hank's balanced salt solution (HBSS), cut into small pieces with sterile scissors, treated with 50 U/ml Dispase (Godo Shusei, Tokyo) for 30–60 min at 37°C in a water bath and, after vigorous pipetting, were allowed to settle. Supernatant fluid containing cell clumps was collected after centrifugation at 100*g*. Cell pellets were washed, resuspended in Dulbecco's modified Eagle's medium (DMEM) (Nissui Pharmaceutical Co., Ltd., Tokyo) containing 10% fetal bovine serum (FBS) (GIBCO, Grand Island, NY) and 100 U/ml penicillin and 100 μg/ml streptomycin and incubated for 1–2 h on plastic dishes at 37°C. Medium containing floating cell clusters was collected and centrifuged. The pellets were resuspended in fresh DMEM with 10% FBS plus serum extender (MITO) (Collaborative Biomedical Products, Bedford, MA) and cultured on plastic dishes in a humidified 5% CO_2 incubator at 37°C with a weekly change of medium.

After several weeks, growing colonies were harvested with trypsin-EDTA (0.125%/2 m*M*) and passaged several times on plastic dishes. Any remaining fibroblasts were removed by mechanical scraping and a differential attachment selection method with trypsin-EDTA, after which cultures of parent cells were obtained (RSC3-P cell line). The RSC3-E2 cell line without metastatic potential after subcutaneous (s.c.) injection into nude mice was selected from RSC3-P cells by single-cell dilution cloning. The RSC3-LM cell line was isolated from a lung metastatic focus in a nude mouse following s.c. injection of RSC3-P cell line and RSC3-E2R cell line similarly following s.c. injection of a RSC3-E2 subline regrown after 5 Gy X-ray irradiation *in vitro* (Fig. 1). These RSC3 series of cell lines have now been cultured for more than 1 year without apparent phenotypic change.

***In vitro* cell growth and invasion assay** To examine the growth rate of RSC3 cell lines *in vitro*, the cells were plated at 1×10^5 cells/35 mm plastic dish in DMEM supplemented with 10% FBS. The number of viable cells was calculated from microscopic observation in triplicate for 4 days after seeding with a hemocytometer.

A modified Boyden chamber invasion assay was performed with polycarbonate filters coated with type I collagen instead of Matrigel separating the upper and lower chambers. FBS was used as a chemoattractant. Cells which had traversed the membrane and spread onto the lower surface of the filter were stained with Giemsa and counted under a microscope.

Tumorigenesis and metastasis in nude mice To examine tumorigenesis of RSC3 cell lines, growing cells were harvested with trypsin-EDTA, and washed with phosphate-buffered saline (PBS), then aliquots of 1×10^6 cells were resuspended in 0.2 ml HBSS and injected s.c. into the left abdominal flanks of 8-week-old male KSN nude mice

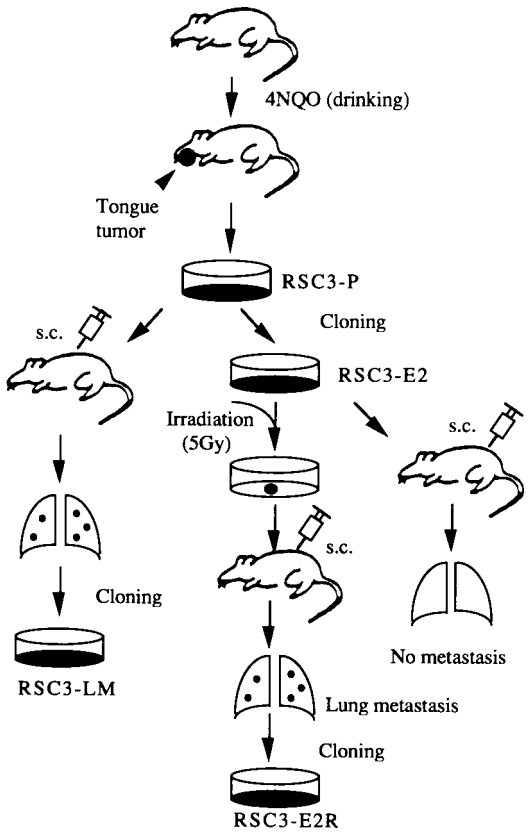

Fig. 1. Schematic representation of isolation procedures for various RSC3 sublines with differing metastatic potential.

(Japan SLC, Inc.). Tumor size was measured in 2 dimensions with a slide caliper every week and estimated from the mean diameter.

KSN mice bearing s.c. tumor were autopsied 4–8 weeks after s.c. injection of cells into the left abdominal flank and the lungs, liver, kidneys, inguinal and para-aortic lymph nodes were removed and fixed in Bouin's solution or 10% formalin solution. The numbers of macroscopic lung metastases were determined by counting visible parietal nodules. Organ metastases were confirmed by histological examination.

Immunofluorescence To examine cellular differentiation, immunostaining of keratin and vimentin was examined. Cultured cells growing in Labtek chamber slides were fixed in cold methanol and treated sequentially with normal swine serum, rabbit anti-keratin polyclonal antibody (DAKO Patts, Copenhagen, Denmark) which recognizes a wide spectrum of keratin and FITC-labeled swine anti-rabbit antibody (DAKO Patts). For vimentin staining, the cells were treated with mouse monoclonal antibody to human vimentin (Sigma, St. Louis, MO) and FITC-labeled rabbit anti-mouse antibody (DAKO Patts). They were viewed with a 20× objective lens using a BX 60 fluorescence microscope (Olympus, Tokyo).

Karyotype analysis Chromosome analysis was performed on metaphase cells treated with 0.01–0.02 μg/ml colcemid for 2 h, subjected to hypotonic conditions for 30 min, then fixed in methanol:acetic acid (3:1). Air-dried slides were G-banded for analysis. At least thirty metaphases were examined for each cell line.

Yeast *p53* functional assay Total RNA was extracted from cultured tumor cells dissolved in ISOGEN (Nippon Gene, Tokyo) with a guanidinium isothiocyanate-phenol-chloroform based method. The yeast rat *p53* functional assay was performed as previously reported.[20] Briefly, RNA was reverse-transcribed at 37°C for 1 h with Moloney murine leukemia virus (MMLV) reverse transcriptase (GIBCO/BRL, Gaithersburg, MD) and 0.5 μM rat *p53* specific primer P1 [5′-AGCCCTAAAGTC-3′]. Rat *p53* cDNA was polymerase chain reaction (PCR)-amplified with Pfu polymerase (Stratagene, La Jolla, CA) and the primer pairs FC2 [5′-CAGCGACAGGGTCACCTAATT-3′] and RC2 [5′-TCAGATGCAGGGCGGTATTT-3′].

The yeast expression vector pLSRP53 for rat[21] was linearized with *Pst*I and *Stu*I and dephosphated with calf intestinal alkaline phosphatase (TaKaRa, Otsu), thus creating gaps between codons 68–193.

Crude PCR products and a linearized *p53*-expression vector were co-transfected into the yeast reporter strain yIG397, which contains an integrated plasmid with the *ADE2* open reading frame under the control of a p53-responsive promoter, and plated and grown at 30°C as previously described.[22] When the strain is transformed with an expression vector encoding wild-type *p53*, the yeast cells express *ADE2* and form white colonies. Otherwise the cells fail to express *ADE2* and form red colonies. To assess the temperature-sensitivity, all samples diagnosed as negative at 30°C were again assessed at 35°C. The percentage of red colonies was obtained by examining more than 200 colonies. For samples with which significant percentages of red colonies were obtained, at least 4 independent yeast colonies were sequenced with a DyeDeoxy Terminator kit (Perkin-Elmer, Norwalk, CT), on an ABI 373A automated sequencer (Applied Biosynthesis, Urayasu).

Statistical analysis The statistical significance of differences in growth was analyzed using Student's *t* test, with $P<0.05$ as the criterion for significance.

RESULTS

Morphological characteristics Primary RSC3 tumors induced by 4NQO in rat tongues were differentiated SCCs with keratin pearl formation (Fig. 4A). Isolation procedures for sublines from this primary tumor are illustrated

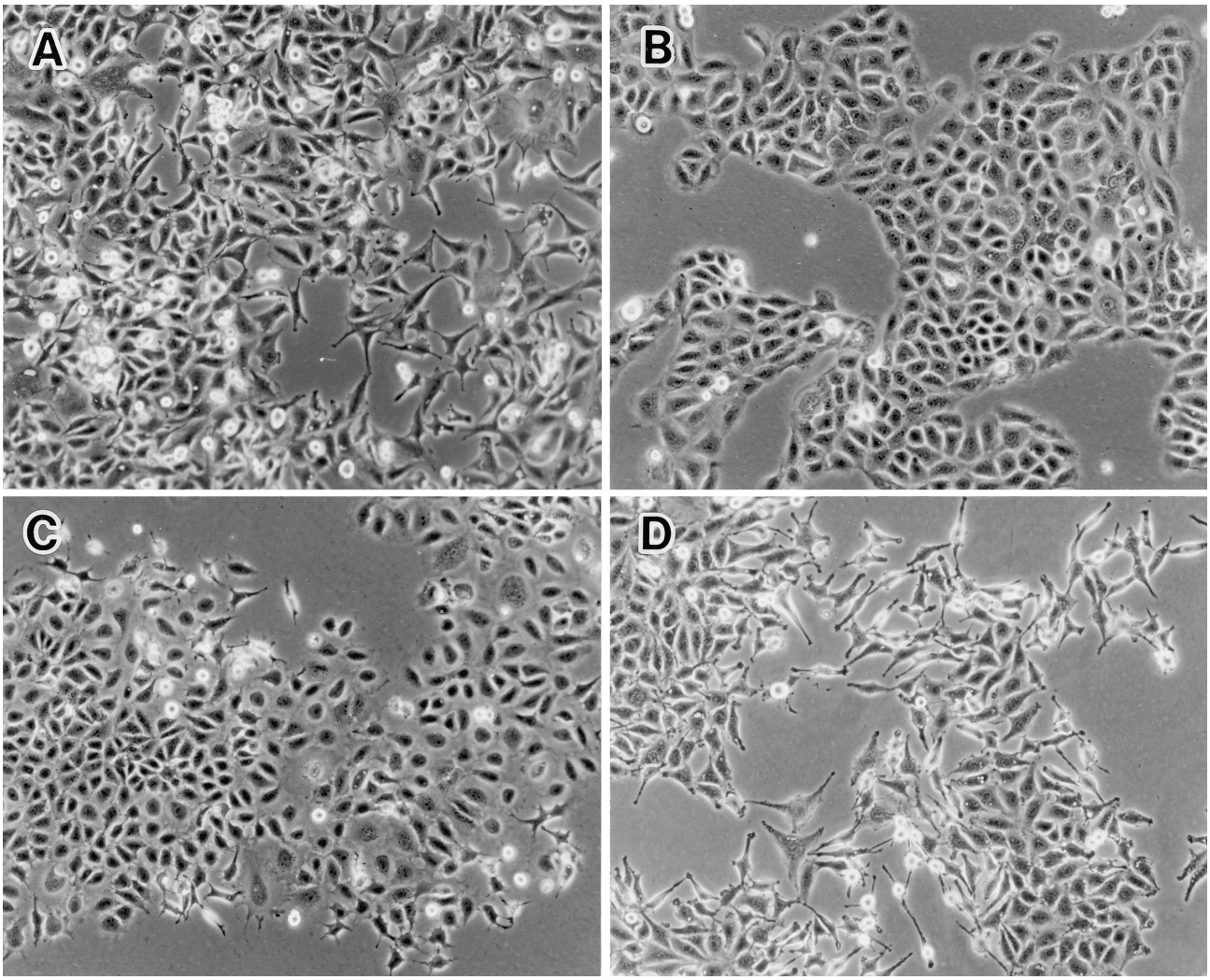

Fig. 2. Phase-contrast photomicrographs of RSC3 cultured cell lines on plastic. Parental RSC3-P cell line (A), RSC3-E2 cell line (B), RSC3-E2R cell line (C) and RSC3-LM cell line (D). RSC3-E2 cells form a typical epithelial monolayer. In contrast, spindle-cell morphology is apparent with RSC3-P and RSC3-LM cells. ×200.

in Fig. 1. The RSC3-P cell line (parent cells) was heterogenous, consisting of spindle cells and polygonal cells in one culture (Fig. 2A). The RSC3-E2 cell line formed typical epithelial monolayers (Fig. 2B), whereas the RSC3-E2R line established from a lung metastatic focus after s.c. injection of radiation-resistant RSC3-E2 cells, showed a stellate morphology (Fig. 2C). Moreover, the RSC3-LM cell line isolated from a lung metastatic focus after s.c. injection of RSC3-P cells showed a spindle-shaped morphology (Fig. 2D). Immunofluorescence microscopy using anti-keratin and anti-vimentin antibody demonstrated the RSC3-E2 cell line to be positive for keratin, whereas RSC3-LM and RSC3-E2R cell lines were negative for keratin and positive for vimentin (Table I).

***In vitro* growth and invasion assay** The growth curves of RSC3 cell lines are shown in Fig. 3A. *In vitro* relative cell growth rates of the RSC3 cell lines on plastic were RSC3-LM>RSC3-E2R>RSC3-P>RSC3-E2. The growth responsiveness to several growth factors was examined using DMEM medium containing 0.2% FBS as the basal medium. Insulin/transferrin and MITO significantly stimulated the growth of all RSC3 cell lines ($P<0.001$), but they proved refractory to basic fibroblast growth factor (bFGF), epidermal growth factor (EGF) and dexamethasone (data not shown). *In vitro* invasion assays demonstrated RSC3-LM cells to be significantly more invasive than the RSC3-E2 and RSC3-E2R lines ($P<0.01$) (Fig. 3B).

Table I. Biological Characteristics of RSC3 Cell Lines

Subline	Clonality	Morphology		Differentiation		Modal chromosome number
		In vitro	*In vivo*	Keratin	Vimentin	
P	Polyclonal	Spindle and stellate	Undifferentiated	–	+	78, 83
LM	Monoclonal	Spindle	Undifferentiated	–	+	83
E2	Monoclonal	Monolayer	Differentiated	+	–	78
E2R	Monoclonal	Stellate	Undifferentiated	–	+	56

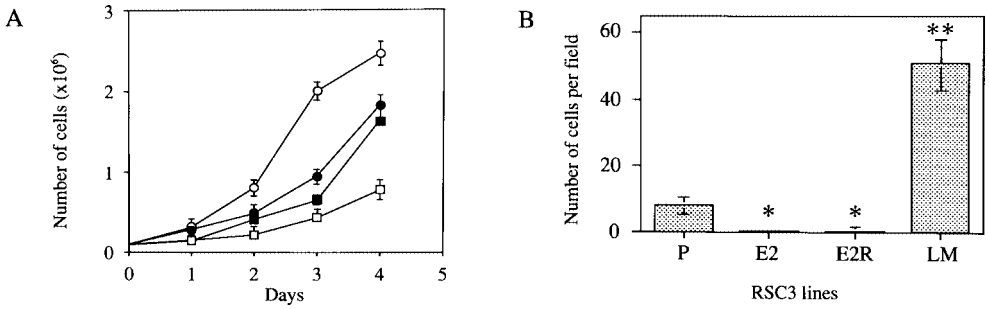

Fig. 3. Results of *in vitro* growth (A) and invasion assays (B) of RSC3 cell lines. (A) Cells (1×10^5) were plated onto 35-mm plastic dishes and cultured. At the indicated times, cells were harvested and counted. Values are means (n=3) ± SD. ○ RSC3-LM, ● RSC3-E2R, ■ RSC3-P, □ RSC3-E2. (B) Cells (2×10^4) were transferred to the upper layer of a Boyden chamber, incubated at 37°C for 12 h and the cells traversed to the lower layer of the membrane were counted after staining. Values represent means±SD of cells per high-power field as determined from 10 representative fields from three replicate filters. * $P<0.05$, ** $P<0.01$ compared to parent cells.

Table II. Tumorigenicity and Spontaneous Metastasis of RSC3 Cell Lines in Nude Mice after Subcutaneous Injection into the Left Abdominal Flanks of Mice

Subline	Growth	Tumorigenicity	Metastasis		
			Lung (average no.)	Lymphnodes	Others
P	Rapid	6/6	4/6 (31)	1/3	ND[a)]
LM	Rapid	5/5	5/5 (58)	2/3	5/5 (Peritoneum)
E2	Slow	5/5	0/6 (0)	0/6	0/6
E2R	Moderate	8/8	7/8 (41)	0/8	5/8 (Kidney)

a) ND, not determined.

Tumorigenicity and metastatic potential in nude mice Findings for tumorigenicity and metastatic potential of RSC3 tumor cells after s.c. injection into nude mice are summarized in Table II. All RSC3 cell lines produced tumors in male nude mice with 100% incidence. Histologically, those observed after s.c. injection of RSC3-E2 cell lines were well-differentiated, keratinizing SCCs (Fig. 4C), similar to the original tongue SCC (Fig. 4A). In contrast, RSC3-LM tumors were undifferentiated spindle-cell tumors (Fig. 4B). RSC3-E2R lesions also had an undifferentiated appearance, but showed some epithelial arrangement or formation of cell nests (Fig. 4D).

The incidences of spontaneous lung metastasis in nude mice receiving s.c. injections of tumor cells were 4/6 (67%) with the RSC3-P cell line, 0/6 (0%) in the RSC3-E2 case, 5/5 (100%) with the RSC3-LM cell line and 7/8

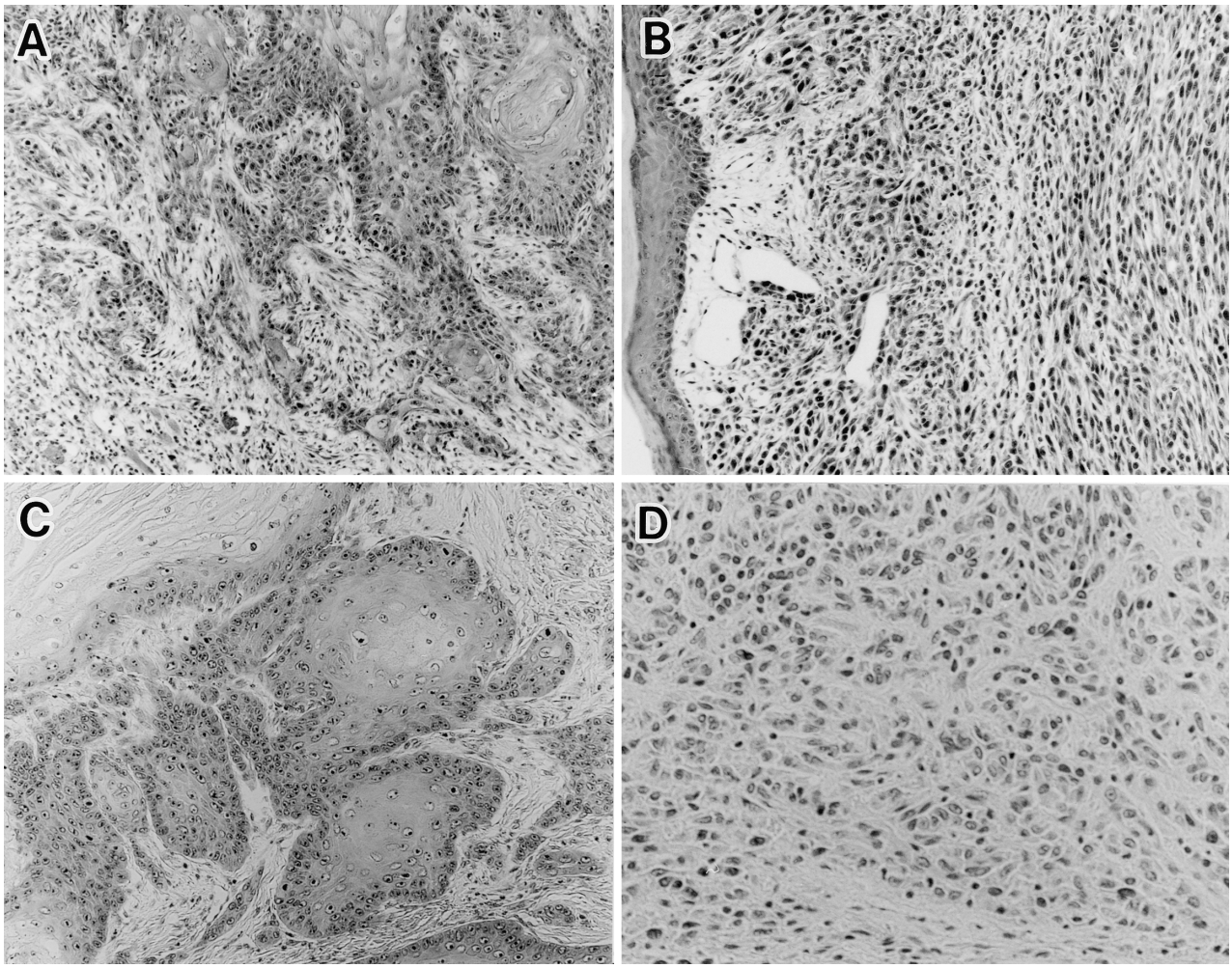

Fig. 4. Histology of the primary tumor induced by 4NQO in the rat tongue (A) and s.c. tumors that developed in nude mice following s.c. injection of RSC3-LM (B), RSC3-E2 (C) and RSC3-E2R (D) cell lines. RSC3-E2 tumors are well-differentiated SCCs with keratinization. In contrast, RSC3-E2R and RSC3-LM tumors are undifferentiated SCCs. Note the spindle tumor appearance of the RSC3-LM tumor. H-E, ×120.

(88%) in the RSC3-E2R case. Average numbers of lung metastatic nodules were more than 30 and the RSC3-LM cell line showed the highest metastatic potential (Fig. 5A). RSC3-P and RSC3-LM cell lines demonstrated inguinal lymphnode metastasis after s.c. injection at a 67% incidence. This spontaneous lymphnode metastasis was usually microscopic (Fig. 5C). Macroscopic popliteal lymphnode metastasis, however, was observed at almost 100% incidence when the RSC3-LM cell line was injected into the foot pads of mice (data not shown). As for metastasis to other organs, RSC3-LM cell lines showed peritoneal metastasis at 5/5 (100%) incidence and RSC3-E2R cell lines metastasized to the kidney at a 63% incidence and to the liver (Table II). Histological features of the lung, lymphnode and other organ metastases were essentially the same as those of the respective primary tumors (Fig. 5, B and C).

Chromosome analysis RSC3-P cell lines had near-tetraploid chromosomes with two peaks of modal chromosome number at 78 and 83. Modal chromosome numbers for the RSC3-E2 and RSC3-LM cell lines were 78 and 83, respectively. RSC3-E2R cell lines had a modal chromosome number of 56, indicating loss of chromosomes due to X-ray irradiation *in vitro* (Table I). Karyotype analysis showed unbalanced $11p^{+}$ translocation as a consistent structural abnormality in all cell lines (Fig. 6).

Detection of *p53* mutations by yeast functional assay A summary of the percentages of red colonies and *p53* clonal

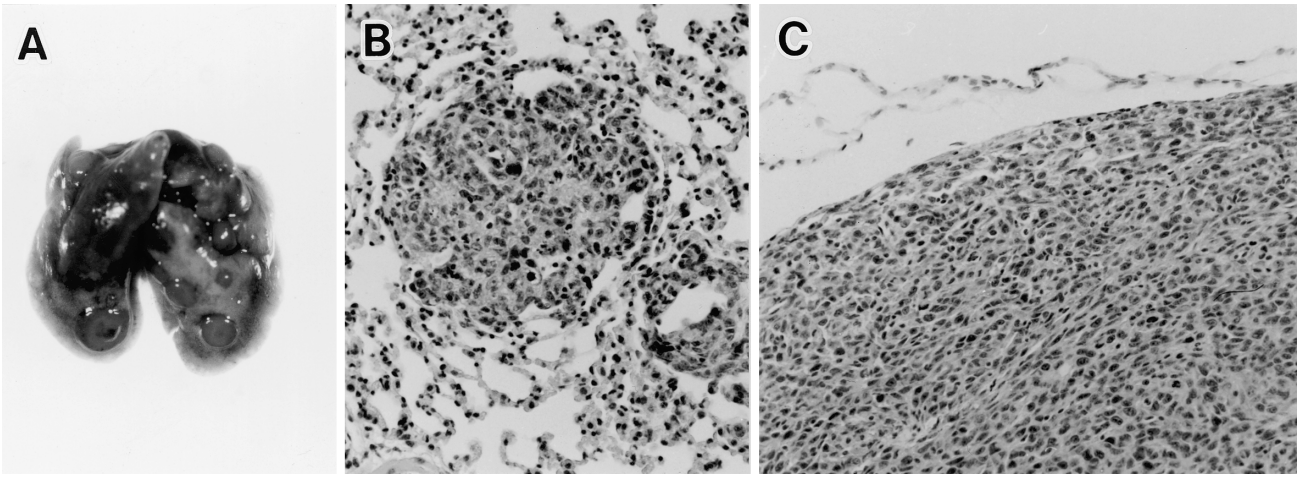

Fig. 5. Lung and lymphnode metastases in nude mice after s.c. injection of tumor cells into the abdominal flank. (A) Metastases in the lung after s.c. injection of RSC3-LM cells. (B) Histology of a metastatic lesion in the lung after s.c. injection of RSC3-E2R cells. H-E, ×40. (C) Histological appearance of a metastasis in an inguinal lymphnode after s.c. injection of RSC3-LM cells. The tumor cells have completely replaced the lymphoid tissue. H-E, ×40.

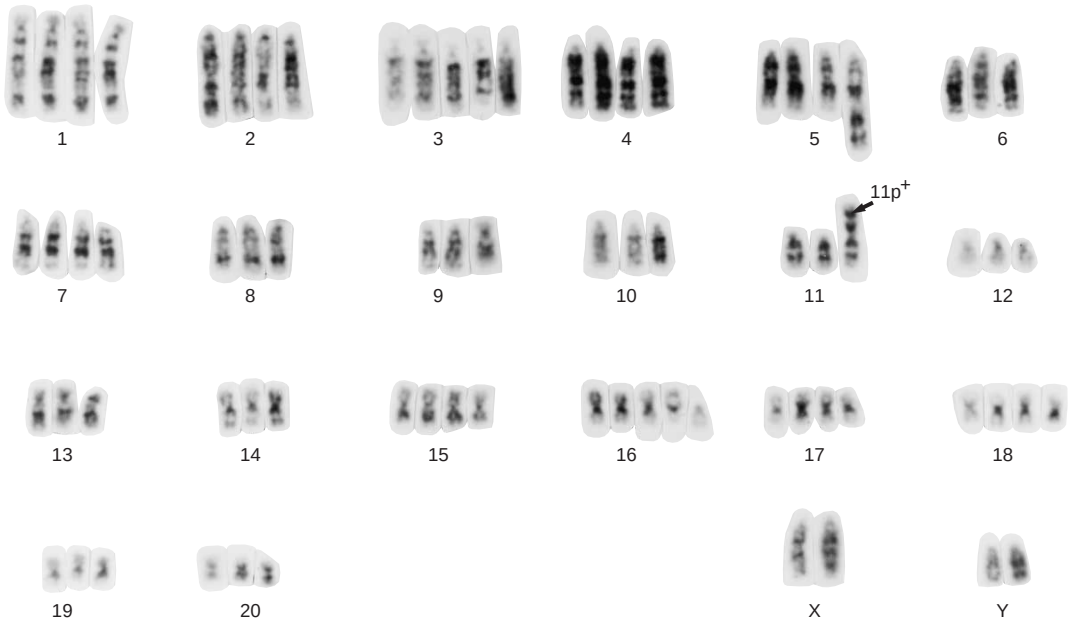

Fig. 6. Representative karyotype of RSC3-LM cells showing 76 XXYY with multiple numerical and structural abnormalities. The chromosome $11p^{+}$ translocation is shared by all the RSC3 cell lines (arrow).

mutations for RSC3 cell lines is shown in Table III. RSC3-P and RSC3-LM cell lines gave 3.0% and 6.5% red colonies at 30°C, and 55% and 50% red colonies at 35°C by yeast functional assay, respectively, indicating the presence of temperature-sensitive mutations at one allele. Sequence analysis revealed the same clonal missense mutation at codon 269 of *p53* exon 8 in both cell lines. The base change was a G-to-A transversion with an amino acid change from glutamine to lysine. On the other hand, RSC3-E2 and RSC3-E2R cell lines gave more than 80% and 90% red colonies at 30°C and 35°C, respectively, suggesting the presence of point mutations with loss of the

Table III. Results of Yeast Functional Assay for *p53* Mutations of RSC3 Cell Lines

Cell line	Percentage red colonies		Clonality of[a] mutations	*p53* mutations			
	30°C	35°C		Codon	Exon	Base change	Amino acid change
P	3.0	55.0	4/8	269	8	GAG → AAG	Glu → Lys
LM	6.5	50.0	6/8	269	8	GAG → AAG	Glu → Lys
E2	84.0	91.0	2/4	106	5	GGC → GTC	Gly → Val
			2/4	170	5	GTC → TTC	Val → Phe
E2R	80.0	92.0	1/6	106	5	GGC → GTC	Glu → Val
			4/6	170	5	GTC → TTC	Val → Phe

a) Mutations were considered clonal when the same mutation was found in at least 2 red colonies sequenced.

wild-type allele. Sequence analysis revealed double mutations consisting of a temperature-sensitive missense mutation at codon 106 and temperature-non-sensitive missense mutation at codon 170 with amino acid changes.

DISCUSSION

For developing a new strategy to treat oral SCC, it is important to understand the molecular bases of tumor progression and metastasis. For this purpose, establishment of appropriate models is essential. To date, however, such human and murine models are quite limited in number and the characterization remains unsatisfactory.[23–25] In the present study, we developed a new series of cell lines from a 4NQO-induced rat tongue SCC. These cell lines are unique for the following two reasons. 1) They consist of both differentiated and undifferentiated SCC components with different degrees of malignancy derived from a single original keratinizing SCC, suggesting that they would be an excellent model for tumor progression from differentiated to undifferentiated, more malignant forms of oral SCC. 2) They are spontaneously metastatic not only by the hematogenous, but also by the lymphogenous route after s.c. injection, with a 100% incidence of lung metastases and a more than 67% incidence of lymphnode metastases, making them suitable for quantitative studies of both types of metastasis.

4NQO-induced SCC cell lines reportedly not infrequently consist of a mixed cellular phenotype with both differentiated and undifferentiated spindle-cell components.[26] In this study, we found the RSC3-E2 cell line to show a typical differentiated SCC phenotype including keratin expression and formation of keratinizing tumors in nude mice, whereas both RSC3-E2R and RSC3-LM cell lines exhibited undifferentiated tumor characteristics such as loss of keratin expression and formation of sarcoma-like tumors. Our results are consistent with those previously reported[17, 18, 26] and indicate phenotypic heterogeneity in 4NQO-induced tongue SCC cell lines, despite derivation from the same original tumors. There are several possible explanations for this phenotypic variation: 1) the original rat tongue tumor consists of heterogenous cellular components including keratinizing SCC as a major component and undifferentiated SCC as a very minor component, and the latter contributes to the generation of undifferentiated sublines because of growth advantages *in vitro*; 2) undifferentiated SCC cell lines are generated from differentiated cell lines by progression with genetic changes during culture; 3) a phenotypic shift from differentiated to undifferentiated cell lines occurs at the epithelial-mesenchymal transition with epigenetic changes during culture[27]; 4) undifferentiated cell lines are contaminating fibroblasts immortalized by 4NQO or spontaneously during culture, possibly derived from the stroma of the primary rat tongue tumor or mouse lung metastasis.

Modal chromosome numbers of RSC3-E2, E2R and LM cell lines were found to be 78, 56 and 83, respectively. The RSC3-E2 and E2R cell lines had the same *p53* mutation pattern, but were different from the LM cell line as demonstrated by the yeast functional assay. However, both RSC3-E2 and LM shared a common karyotype aberration on chromosome 11. These findings strongly suggest that E2R was generated *in vitro* from the E2 cell line by radiation-induced genetic changes, including loss of chromosomes, and that LM was not generated as a consequence of epithelial-mesenchymal transition of E2. Also, involvement of contaminating fibroblasts derived from either stroma of the original tumor or mouse lung therefore appears unlikely. In fact, chromosomes of LM cell line were metacentric, confirming the cell line to be of rat origin and not from fibroblasts of nude mouse origin. Moreover, Patel *et al.* reported that 4NQO-induced rat oral keratinocyte cell lines, including both differentiated SCC and undifferentiated spindle-cell lines shared common structural abnormalities such as $10q^+$ and $11p^+$ translocation,[18] as in our RSC3 cases, indicating the same clonal origin of differentiated and undifferentiated SCC. It is therefore most likely that the LM cell line was not contaminating 4NQO-transformed fibroblasts, but was generated from progenitor cells of differentiated SCC compo-

nent present predominantly in the original tongue tumor during 4NQO-induced carcinogenesis or an early stage of subsequent progression.

Generation of two independent undifferentiated cell lines *in vitro* and *in vivo* (RSC3-E2R and LM) from differentiated SCC suggests that 4NQO-induced differentiated SCCs are relatively unstable in terms of epithelial phenotype and tend to progress to undifferentiated phenotype via different genetic pathways. It was reported that chromosome 3 and 12 aberrations were seen in undifferentiated spindle tumor cells but not differentiated cells of 4NQO-induced rat oral SCCs and suggested that proto-oncogenes and/or tumor suppressor genes located on chromosomes 3 and 12 may control tumor cell differentiation and progression.[18] Our 4NQO-induced SCC model, however, did not demonstrate such chromosome 3 and 12 abnormalities, again confirming that tumor progression can occur not through a single common pathway, but through multiple genetic pathways, probably depending on non-specific chromosome damage by 4NQO,[28] unlike hot-spot loci induced by 3,4-benzpyrene and 9,10-dimethyl-1,2-benzanthracene.[29, 30] Similar phenotypic shifts during serial passages *in vivo* and *in vitro* have also been observed for spontaneous and chemically induced rat mammary carcinomas and prostatic carcinomas.[31–33]

Another interesting feature of the presently described cell lines is the heterogeneity of metastatic potential with non-metastatic (E2), hematogenously metastatic (E2R) and both hematogenously and lymphogenously metastatic (LM) phenotypes. Undifferentiated spindle tumor cells are well recognized to be aggressive and to have a poor prognosis in human and rodent oral SCCs.[6, 17] Our undifferentiated cell lines (RSC3-LM and RSC3-E2R) showed more rapid growth and higher metastatic potential than the differentiated RSC3-E2 cell line, consistent with those previously reported, but the patterns of metastasis clearly differed between the two. RSC3-LM cells with spindle phenotype are highly aggressive and exhibit both invasion and metastasis, including muscle invasion and peritoneal metastasis. In contrast, RSC3-E2R cells with non-spindle morphology show only hematogenous metastasis and no invasion. In agreement with this *in vivo* behavior, RSC3-LM cells but not RSC3-E2R cells demonstrated strong invasiveness in the *in vitro* invasion assay. Moreover, active forms of MMP-2 and MMP-9 were observed only in RSC3-LM cells (unpublished results). These results strongly suggest that hematogenous and lymphogenous metastasis by RSC3-LM cells is invasion-dependent, but hematogenous metastasis by RSC3-E2R cells is invasion-independent. In this respect, it is of note that RSC3-E2R cells have an undifferentiated appearance, but retain some epithelial characteristics such as formation of cell nests and basement membrane (BM), even if it is incomplete (unpublished result), suggesting that they should actually be classified as poorly differentiated. Consistent with our present results, metastatic and non-metastatic variants of Lewis lung carcinoma both showed an undifferentiated appearance, but only a metastatic line retained some ability for BM formation.[34] Therefore, BM formation by tumor cells may be a phenotype which is related to invasion-independent metastasis. Further studies on the molecular mechanisms underlying invasion-independent hematogenous metastasis in RSC3-E2R cells are now under way in our laboratory.

In conclusion, three cell lines isolated from a 4NQO-induced rat tongue SCC in the present study demonstrate distinct characteristics, not observed in previous studies of 4NQO-induced rat oral SCC cell lines, in terms of tumor progression, metastatic potential and genetic alterations. These cell lines may be relevant to human oral SCCs and provide a useful model for analyzing genetic changes related to the tumor progression from differentiated SCCs to undifferentiated spindle-cell forms and for investigating molecular mechanisms of hematogenous and lymphogenous metastasis.

ACKNOWLEDGMENTS

We are grateful to H. Fukami and M. Yamada for expert technical assistance. This work was supported in part by a Grant-in-Aid for Scientific Research from the Ministry of Education, Science, Sports and Culture, Japan.

(Received May 15, 2000/Revised August 15, 2000/Accpeted August 22, 2000)

REFERENCES

1) Parkin, D. M., Pisani, P. and Ferlay, J. Estimates of the worldwide incidence of eighteen major cancers in 1985. *Int. J. Cancer*, **54**, 594–606 (1993).
2) Boring, C. C., Squires, T. S. and Tong, T. Cancer statistics 1991. *Cancer*, **41**, 1–11 (1991).
3) Clavel, M. and Maged Mansour, A. R. Head and neck cancer: prognostic factors for response to chemotherapy. *Eur. J. Cancer*, **27**, 349–356 (1991).
4) Leemans, C. R., Tiwari, R., Nauta, J. J., van der Waal, L. and Snow, G. B. Regional lymph node involvement and its significance in the development of distant metastases in head and neck carcinoma. *Cancer*, **71**, 452–456 (1993).
5) Yamamoto, E., Miyakawa, A. and Kohama, G. Mode of invasion and lymph node metastasis in squamous cell carcinoma of the oral cavity. *Head Neck Surg.*, **6**, 938–947 (1984).
6) Ellis, G. L. and Corio, R. L. Spindle cell carcinoma of the oral cavity. A clinicopathological assessment of fifty-nine

cases. *Oral Surg.*, **50**, 523–534 (1980).
7) Takata, T., Ito, H., Ogawa, I., Miyauchi, M., Ijuhin, N. and Nikai, H. Spindle cell squamous carcinoma of the oral region. Immunohistochemical and ultrastructural study on the histogenesis and differential diagnosis with a clinicopathological anaysis of six cases. *Virchows Arch. A Pathol. Anat. Histopathol.*, **419**, 177–182 (1991).
8) Matsui, T., Ota, T., Ueda, Y., Tanino, M. and Odashima, S. Isolation of a highly metastatic cell line to lymph node in human oral squamous cell carcinoma by orthotopic implantation in nude mice. *Oral Oncol.*, **34**, 253–256 (1998).
9) Kawamata, H., Nakashiro, K., Uchida, D., Harada, K., Yoshida, H. and Sato, M. Possible contribution of active MMP2 to lymph-node metastasis and secreted cathepsin L to bone invasion of newly established human oral-squamous-cancer cell lines. *Int. J. Cancer*, **70**, 120–127 (1997).
10) Iida, K., Yamamoto, M., Kato, M., Yosha, K., Kurita, K. and Tatematsu, M. Strong expression of glutathione S-transferase placental form in early preneoplastic lesions and decrease with progression in hamster buccal pouch carcinogenesis. *Cancer Lett.*, **135**, 129–136 (1999).
11) Vengadesan, N., Aruna, P. and Ganesan, S. Characterization of native fluorescence from DMBA-treated hamster cheek pouch buccal mucosa for measuring tissue transformation. *Br. J. Cancer*, **77**, 391–395 (1998).
12) Crane, I. J., Luker, J., Stone, A., Scully, C. and Prime, S. S. Characterization of malignant rat keratinocytes in culture following the induction of oral squamous cell carcinomas *in vivo*. *Carcinogenesis*, **7**, 1723–1727 (1986).
13) Crane, I. J., Luker, J., de Gay, L., Rice, S. Q., Stone, A., Scully, C. and Prime, S. S. Transformation of oral keratinocytes *in vitro* by 4-nitroquinoline N-oxide. *Carcinogenesis*, **9**, 2251–2256 (1988).
14) Crane, I. J., Patel, V., Scully, C. and Prime, S. S. Development of aneuploidy in experimental oral carcinogenesis. *Carcinogenesis*, **10**, 2375–2377 (1989).
15) Witjes, M., Scholma, J., van Drunen, E., Roodenburg, J. L., Mesander, G., Hagemeijer, A. and Tomson, A. M. Characterization of a rat oral squamous cell carcinoma cell line UHG-RaC ′93 induced by 4-nitroquinoline-1-oxide *in vivo*. *Carcinogenesis*, **16**, 2825–2832 (1995).
16) Game, S. M., Stone, A., Matthews, J. B., Scully, C. and Prime, S. S. Differentiation of malignant oral rat keratinocytes reflects changes in EGF and TGF-beta receptor expression but not growth factor dependence. *Carcinogenesis*, **12**, 409–416 (1991).
17) Davies, M., Prime, S. S., Stone, A. M., Heung, Y. L., Huntley, S. P., Matthews, J. B., Eveson, J. W. and Paterson, I. C. Overexpression of autocrine TGF-beta 1 suppresses the growth of spindle epithelial cells *in vitro* and *in vivo* in the rat 4NQO model of oral carcinogenesis. *Int. J. Cancer*, **26**, 68–74 (1997).
18) Patel, V., Poulopoulos, A. K., Levan, G., Game, S. M., Eveson, J. W. and Prime, S. S. Loss of expression of basement membrane proteins reflects anomalies of chromosomes 3 and 12 in the rat 4-nitroquinoline-N-oxide model of oral carcinogenesis. *Carcinogenesis*, **16**, 17–23 (1995).
19) Ohne, M., Satoh, T., Yamada, S. and Takai, H. Experimental tongue carcinoma of rats induced by oral administration of 4-nitroquinoline 1-oxide (4NQO) in drinking water. *Oral Surg. Oral Med. Oral Pathol.*, **59**, 600–607 (1985).
20) Yamamoto, K., Nakata, D., Tada, M., Tonoki, H., Nishida, T., Hirai, A., Ba, Y., Aoyama, T., Hamada, J., Furuuchi, K., Harada, H., Hirai, K., Shibahara, N., Katsuoka, Y. and Moriuchi, T. A functional and quantitative mutational analysis of p53 mutations in yeast indicates strand biases and different roles of mutations in DMBA- and BBN-induced tumors in rats. *Int. J. Cancer*, **83**, 700–705 (1999).
21) Ba, Y., Tonoki, H., Tada, M., Nakata, D., Hamada, J. and Moriuchi, T. Transcriptional slippage of p53 gene enhanced by cellular damage in rat liver: monitoring the slippage by a functional assay. *Mutat. Res.*, **447**, 209–220 (2000).
22) Yamamoto, S., Tada, M., Lee, C. C. R., Masuda, C., Wanibuchi, H., Yoshimura, R., Wada, S., Yamamoto, K., Kishimoto, T. and Fukushima, S. p53 status in multiple human urothelial cancers: assessment for clonality by the yeast p53 functional assay in combination with p53 immunohistochemistry. *Jpn. J. Cancer Res.*, **91**, 181–189 (2000).
23) Okumura, K., Konishi, A., Tanaka, M., Kanazawa, M., Kogawa, K. and Niitsu, Y. Establishment of high- and low-invasion clones derived from a human tongue squamous-cell carcinoma cell line SAS. *J. Cancer Res. Clin. Oncol.*, **122**, 243–248 (1996).
24) Momose, F., Araida, T., Negishi, A., Ichijo, H., Shioda, S. and Sasaki, S. Variant sublines with different metastatic potential selected in nude mice from human oral squamous cell carcinomas. *J. Oral Pathol. Med.*, **18**, 391–395 (1989).
25) Morifuji, M., Taniguchi, S., Sakai, H., Nakabeppu, Y. and Ohishi, M. Differential expression of cytokeratin after orthotopic implantation of newly established human tongue cancer cell lines of defined metastatic ability. *Am. J. Pathol.*, **156**, 1317–1326 (2000).
26) Game, S. M., Stone, A., Scully, C. and Prime, S. S. Tumour progression in experimental oral carcinogenesis is associated with changes in EGF and TGF-beta receptor expression and altered responses to these growth factors. *Carcinogenesis*, **11**, 965–973 (1990).
27) Valles, A., Boyer, B., Badet, J., Tucker, G., Barritault, D. and Thiery, J. P. Acidic fibroblast growth factor is a modulator of epithelial plasticity in a rat bladder carcinoma cell line. *Proc. Natl. Acad. Sci. USA*, **87**, 1124–1128 (1990).
28) Kondo, S. Molecular biology of 4-nitroquinoline 1-oxide in the prokaryotic system. *In* "The Nitroquinolines," ed. T. Sugimura, pp. 47–64 (1981). Raven Press, New York.
29) Levan, A., Levan, G. and Mitelman, F. Chromosomes and cancer. *Hereditas*, **86**, 15–30 (1977).
30) Mitelman, F. and Levan, G. The chromosome of primary 7, 12-dimethyl(a)anthracene-induced rat sarcoma. *Hereditas*, **71**, 325–334 (1972).
31) Aldaz, C. M., Chen, A., Gollahon, L. S., Russo, J. and Zappler, N. Nonrandom abnormalities involving chromo-

some 1 and Harvey-ras-1 alleles in rat mammary tumor progression. *Cancer Res.*, **52**, 4791–4798 (1992).
32) Lee, C., Lapin, V., Oyasu, R. and Battifora, H. Effect of ovariectomy on serially transplanted rat mammary tumors induced by 7,12-dimethylbenzanthracene. *Eur. J. Cancer Clin. Oncol.*, **17**, 801–808 (1981).
33) Nakanishi, H., Taylor, R. M., Chrest, F. J., Masui, T., Utsumi, K., Tatematsu, M. and Passaniti, A. Progression of hormone-dependent adenocarcinoma cells to hormone-independent spindle carcinoma cells *in vitro* in a clonal spontaneous rat mammary tumor cell line. *Cancer Res.*, **55**, 399–407 (1995).
34) Nakanishi, H., Takenaga, K., Oguri, K., Yoshida, A. and Okayama, M. Morphological characteristics of tumours formed by Lewis lung carcinoma-derived cloned cell lines with different metastatic potentials: structural differences in their basement membranes formed *in vivo*. *Virchows Arch. A Pathol. Anat. Histopathol.*, **420**, 163–170 (1992).